Interaction of surfaces in smectic membranes and their instability near thinning transitions

P. V. Dolganov,[1] P. Cluzeau,[2] G. Joly,[3] V. K. Dolganov,[1] and H. T. Nguyen[2]
[1]*Institute of Solid State Physics, Russian Academy of Sciences, 142432 Chernogolovka, Moscow Region, Russia*
[2]*Centre de Recherches Paul Pascal, CNRS, Université de Bordeaux I, Avenue A. Schweitzer, F-33600 Pessac, France*
[3]*Laboratoire de Dynamique et Structures des Matériaux Moléculaires, UMR CNRS 8024, Université de Lille 1, 59655 Villeneuve d'Ascq Cedex, France*

(Received 22 April 2005; published 26 September 2005)

We report measurements of the interaction between surfaces of the presmectic membrane above the temperature of transition to the phase without layer ordering. Investigations were performed employing cholesteric droplets embedded in the membrane in the temperature range of thinning transitions. Upon heating, the difference between the membrane tension and surface tension of the bulk sample decreases sufficiently, which leads to membrane instability. After the thinning transition, the membrane returns to a stable state with a larger value of surface interaction.

DOI: 10.1103/PhysRevE.72.031713 PACS number(s): 64.70.Md, 61.30.−v

Competition between surface and bulk behavior leads to unusual physical properties of free-standing smectic membranes [1,2]. Smectic layers in membranes are parallel to the free surfaces. Every layer is a two-dimensional (2D) fluid formed by elongated molecules. In the smectic-*A*(Sm*A*) phase, long molecular axes orient perpendicular to the layer plane, while in the smectic-*C*(Sm*C*)-type phases, long molecular axes tilt with respect to the layer normal. High structure quality, possibility to prepare membranes with exact numbers of smectic layers (from two to more than a thousand) make these membranes very suitable objects for investigations of surface effects, 2D phenomena, and phase transitions in confined geometry [1,2].

In 1994 Stoebe, Mach, and Huang [3] found layer-by-layer thinning transitions of smectic membranes. This phenomenon is one of the most prominent demonstrations of the competition between surface and bulk behavior. Above the bulk Sm*A*-isotropic (*I*) transition temperature T_b, membranes do not melt. Smectic ordering is retained up to the temperature $T_N > T_b$ at which membrane thickness decreases by one layer. T_N increases with decreasing membrane thickness so with heating the membrane undergoes the step-by-step thinning transitions. Since the pioneering paper of Stoebe *et al.* [3], in the past decade, this phenomenon has been intensively investigated both experimentally [4–11] and theoretically [12–19]. It was established that thinning transitions are typical in membranes consisting of materials with phase transitions between smectic structures and phases without layer ordering. Thinning was observed for different low temperature smectic structures (Sm*A*, Sm*C*, ferroelectric SmC^*) and high temperature nonlayered phases [nematic, cholesteric (N^*), *I*]. Thinning transitions are possible due to the surface ordering effect. Above the bulk transition temperature, the formation of smectic layers was observed on the free surface [20] and near the solid substrate [21].

Theories based on de Gennes presmectic [14–16,18,19,22], density-functional [13], and McMillan [12,17] models were used for quantitative description of the membrane structure, temperature dependence, and the mechanism of thinning. According to the presmectic model [14,15], the free energy exhibits a sequence of metastable minima for the smectic state at all temperatures. However, upon heating at some critical temperature, which depends on the thickness, the membrane becomes unstable. Instability arises from the small value of the smectic order parameter in the middle plane of the membrane. In an unstable regime, the compression modulus tends to zero and the large elastic deformation is located in the central layers, which allows the membrane to decrease its thickness through the nucleation of the dislocation loops. According to the modified presmectic theory [16,18,19], a maximum temperature T_{CN} exists above which the discrete free-energy wells vanish for films with $N > N_C$. This temperature is the upper limit for thinning transition. Both in phenomenological presmectic and other models, the instability of the layer structure and its stabilization after thinning are related to the change of membrane energy upon heating—more precisely, to the change of the membrane tension. Theories predict the change of surface interaction in membranes upon approaching and throughout the thinning transition. Although the surface interaction energy constitutes a small part of the membrane tension, it is essential for the behavior of membranes and their physical properties. In recent years, the interaction of surfaces was shown to play a crucial role in wetting phenomena, stability of films, and their behavior in an external field [23].

In this paper, we report the measurements of the surface interaction in the membrane, namely, the difference between the membrane tension τ_N and the tension of the bulk sample $\tau_b \tau_b = 2\gamma$, γ is the surface tension) in the temperature range of membrane instability and thinning transitions. We found that $(\tau_N - \tau_b)/\tau$ increases with heating and approaches zero [here $\tau = (\tau_N + \tau_b)/2$]. The small difference between τ_N and τ_b in the presmectic membrane at a high temperature leads to membrane instability and thinning transitions. Decreasing of the number of smectic layers at the thinning transition leads to stepwise decreasing $\tau_N - \tau_b$ (due to the decrease of the membrane tension τ_N) on the value of order $3 \times 10^{-3}\tau$ and allows the stabilization of the layer structure of the membrane.

The membranes studied were composed from smectic material *S*-4′-undecyloxybiphenyl-4-yl 4-(1-methylheptyloxy) benzoate (11BSMHOB) [24]. In a bulk sample, 11BSMHOB exhibits the following phase sequence: SmC^* − 108 °C − N^* − 123.9 °C − I. The tilt angle in the SmC^* phase is nearly constant and remains about 45° at the first-order SmC^*-N^* phase transition. The membranes of uniform thickness were prepared by drawing the material in the SmC^* phase across a circular hole (4 mm diameter) in a thin glass plate. In our experiments, we studied membranes from 15 to 21 smectic layers. The thickness of the membranes was determined from the spectral dependence of the optical reflection in the "backward" geometry [25]. Investigations of cholesteric droplets nucleated in the presmectic membrane [26–28] enabled us to obtain information on membrane tension [29]. The diameter of droplets was from 15 to 35 μm. The droplet profile was determined from the position of interference fringes in droplets [26–29] in reflected monochromatic light ($\lambda = 500$ nm). The images of the membranes and droplets were recorded using light reflection microscopy and a charge-coupled device camera.

In the past years, different methods were used to determine the membrane tension: the measurements of curvature of a flexible string on the membrane boundary [30], the resonant frequencies of membrane vibrations [31], the force of a membrane drawn between two circular edges [32], the contact angle between a membrane and its meniscus [15,33], and the curvature of membrane under pressure [34]. The precision of the measurements was increased by about two orders, which allowed us to obtain several principal results. Membrane tension decreases with temperature below the bulk transition temperature and its value is lower in thinner membranes [32]. Above the bulk transition, the membrane tension increases with temperature and abruptly decreases at thinning transitions [34]. In order to determine the surface interaction in the membrane in the temperature range of thinning transitions, we used a precise method based on the measurement of the droplet geometry in the smectic membrane [29]. The droplet shape is very sensitive to the small difference between the membrane tension and the surface tension of the bulk sample. This allows us to detect small effects ($|\tau_N - \tau_b| / \tau \lesssim 10^{-3}$). In 11BSMHOB, some quantity of cholesteric droplets nucleates just above the temperature of the bulk SmC^*-N^* phase transition T_c and preserves after membrane thinning, which enables the measurements to be made below and above the temperatures of the thinning transitions. On cooling below T_c, the droplets form flat SmC^* islands thicker than the background membrane. The transformation between N^* droplets and smectic islands is reversible and occurs approximately near T_c. Above T_c the cholesteric phase is stable. Note also that all free-standing film states are metastable [2,35] and $\tau_{N+1} > \tau_N$ [32]. These are the reasons why above T_c the material contained in droplets does not spread throughout the membrane and make it thicker.

Figure 1 shows the dependence of the relative droplet diameter D/D_0 on temperature for films of different thicknesses (D_0 is the droplet diameter at temperature $T = T_N - 1.3$ °C). Droplet diameter increases with temperature

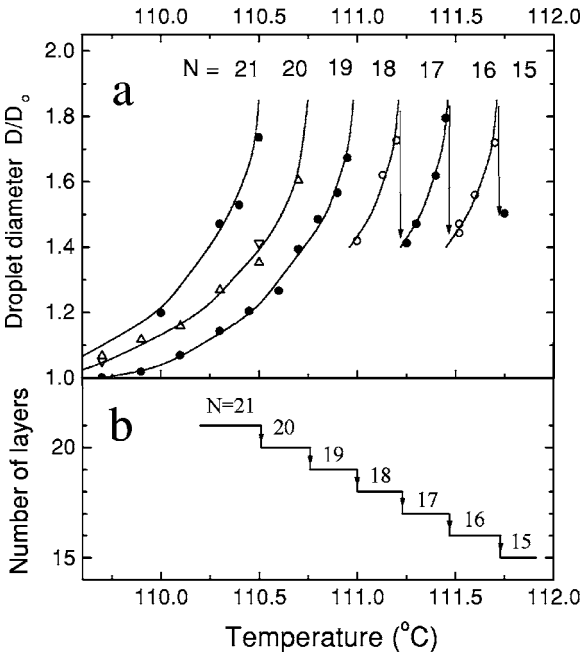

FIG. 1. (a) Dependence of the relative droplet diameter D/D_0 on the temperature for the droplets in membranes of different thicknesses. D_0 is the droplet diameter at the temperature $T_0 = T_N - 1.3$ °C; T_N—temperature of thinning transition; N—number of smectic layers in the membrane. The droplet diameter increases on heating and stepwisely decreases at the thinning transitions. (b) The temperature regions of existence of N-layer films when the thinning transitions occur.

(Fig. 1). Succeeding cooling leads to the decrease of the droplet diameter. The slope of each curve increases, essentially approaching the thinning transition temperature. Data in the temperature interval 111.0 °C to 111.75 °C was obtained during a thinning transition run for the same film. The film thickness decreases from $N = 18$ to $N = 15$ layers over the layer-by-layer thinning process. The droplet diameter increases with temperature and then stepwisely decreases at every thinning transition. The droplet profile was determined from the position of black and bright fringes inside the droplet, which result from the interference of light reflected from the top and bottom of the droplet [26–29]. Figure 2 shows the form of droplets in a 16-layer membrane at two temperatures that differ only by 0.18 °C (111.52 °C, full circles; 111.7 °C, open circles). Heating leads to the increase of the droplet diameter and the decrease of its thickness so that the droplet volume remains nearly constant. The droplet shape may be approximated by two spherical caps [29]. In a small temperature interval near thinning transition (Fig. 2), their radius increases from about 180 μm to 340 μm. We may conclude that droplets exhibit critical behavior near the thinning transitions.

The droplet geometry in the smectic membrane is determined by competition between the membrane tension and surface tension of the droplet [29]. Schematic representation of a droplet is shown in Fig. 3. Two surfaces confining a droplet consist of smectic layers parallel to free surfaces (Fig. 3). Layer ordering penetrates into the droplet on the distance of the surface penetration length ξ. The number of

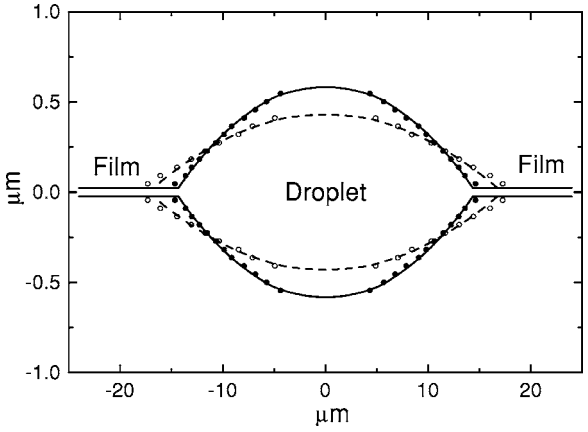

FIG. 2. The droplet shape in the membrane with a number of smectic layers $N=16$. $T=111.52$ °C (solid circles), $T=111.7$ °C (open circles). Solid curves are the spherical caps with $R=182$ μm, $H=1.2$ μm. Dashed curves correspond to $R=343$ μm, $H=0.87$ μm.

smectic layers near the free surface decreases with temperature [20]. The surface layer ordering gives the smectic contribution to the surface tension. The total energy $F=F_M+F_D$ of the system consists of membrane $F_M=\tau_N S_M$ and surface droplet $F_D=\tau_b S_D$ energies, where $S_M=S_0-\pi D^2/4$ and $S_D=\pi(D^2+H^2)/2$ are membrane and droplet areas, S_0 is the area of membrane without the droplet, and H is the droplet height. We neglect the small change of surface area in the place of contact between the membrane and the droplet. Minimization of energy F with respect to D and H under the condition of a constant droplet volume $V=\pi H(3D^2+H^2)/24$ gives [29]

$$(\tau_N-\tau_b)/\tau \approx -2(H/D)^2. \tag{1}$$

If the droplet volume is the same at different temperatures, dependence $(\tau_N-\tau_b)/\tau$ on D reads

$$(\tau_N-\tau_b)/\tau \approx -(128V^2/\pi^2)D^{-6}. \tag{2}$$

Equation (1) can be rewritten in the following form:

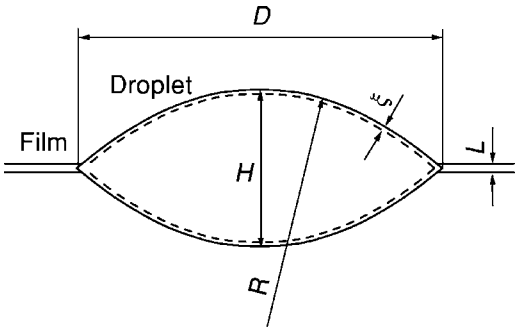

FIG. 3. Sketch of the droplet in the smectic membrane. L is the membrane thickness; R—radius of spherical cap; ξ—surface penetration length of smectic ordering.

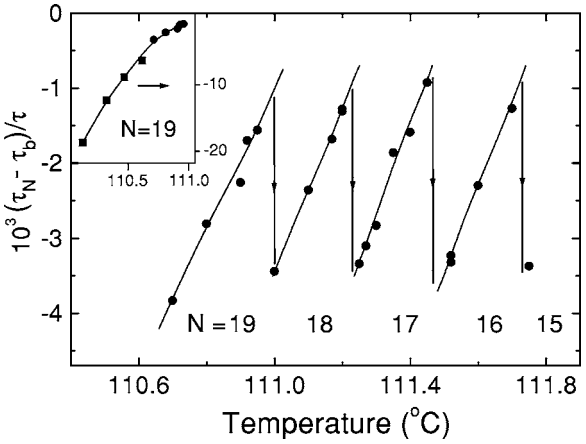

FIG. 4. Relative difference $(\tau_b-\tau_N)/\tau$ between the membrane tension and the surface tension of the bulk sample versus temperature for membranes of different thickness N. Arrows show the stepwise change of $(\tau_b-\tau_N)/\tau$ at the thinning transitions. Solid squares in the inset of the figure represent the data for a 19-layer membrane in a wide range of $(\tau_b-\tau_N)/\tau$ (right axis).

$$(\tau_N-\tau_b)/\tau \approx -\theta_M^2/2, \tag{3}$$

where θ_M is the apparent matching angle between the droplet and membrane surfaces. This equation can be obtained immediately from the Young equation for the apparent matching angle between the membrane and the droplet. In this form, the relation between $(\tau_N-\tau_b)/\tau$ and the droplet parameters is similar to the relation obtained in [15] for the determination of membrane characteristics from the profile of the meniscus.

Figure 4 shows $(\tau_N-\tau_b)/\tau$ for the membranes of different thicknesses. Near the temperature of thinning transitions, the data were obtained using Eq. (1) and fitting the experimental droplet profile by a circular arc (Fig. 2). Determination of $(\tau_N-\tau_b)/\tau$ from a matching angle [Eq. (3)] gave the results with an accuracy of about 10% coinciding with data of Fig. 4. It is worth noting that measurements of the droplet profile allow us to determine both the ratio (H/D) and the apparent matching angle θ_M with high precision. This enabled us to perform measurements for the first time in the temperature region of the thinning transitions. At temperatures "far" from the thinning transitions, droplets do not show discrete interference fringes. Due to the increase of surface curvature of droplets with decreasing temperature, the distance between the interference fringes decreases and becomes less than microscope resolution. Data in a broader region (solid squares in the inset of Fig. 4) were obtained from Eq. (2) under the assumption that the droplet volume remained constant. We found that $(\tau_N-\tau_b)/\tau$ displays oscillations throughout the thinning transitions (Fig. 4). Between successive thinning transitions, $(\tau_N-\tau_b)/\tau$ increases with temperature. At thinning transitions, $(\tau_N-\tau_b)/\tau$ stepwisely decreases.

Typical values of the membrane tension are about 25–60 dyn/cm [30–32]. The main contribution γ_0 to surface tension γ is connected with the formation of the condensed state (liquid or nematic). Contributions to γ from periodic

smectic ($\gamma=\gamma_0+\gamma_S$) or crystal ($\gamma=\gamma_0+\gamma_C$) ordering are small even at low temperature. In the usual crystals, $\gamma_C>0$ (crystal melting starts from the surface) and "precrystal" films do not exist. In smectics, γ_S and the fluctuation profile depend upon the ratio $\nu=\gamma/(BK)^{1/2}$, where B is the elastic constant associated with layer compressions, and K is the elastic constant associated with layer undulations [2]. For $\nu>1$, the surface damps the fluctuations, while for $\nu<1$, the fluctuation amplitudes are enhanced at the surfaces. Above the bulk transition temperature, γ_S remains finite and negative up to T_S as long as smectic ordering exists near the surface. The difference T_S-T_c is about 10 °C [20]. However, the presmectic membrane can exist even above T_S due to the interaction between the two surfaces, which induces smectic ordering in the thin membrane. In SmC^*, τ depends, in particular, on the tilt angle. In 11BSMHOB, the tilt angle is nearly constant with temperature. The contribution of the smectic elasticity to membrane tension is very small at low temperature. Above T_c, the compression energy becomes more important [19]. Membrane tension $\tau_N(\tau_\infty=2\gamma)$ can be divided in two parts related with nonstructural (τ_{0L}) and structural (τ_{SN}) tension $\tau_N=\tau_{0L}+\tau_{SN}$. In our experiments, we measured the excess energy $(\tau_N-\tau_b)/\tau$ (Fig. 4) resulting from a finite thickness of the membrane and interaction between surfaces F_{in}. In the common case, $(\tau_N-\tau_b)$ consists of two parts

$$\tau_N-\tau_b=(\tau_{0L}-2\gamma_0)+(\tau_{SN}-2\gamma_S). \tag{4}$$

Nonsmectic interaction (first term) is usually attributed to the van der Waals attraction between surfaces $F_W=-A/12\pi L^2$ [36], where A is the Hamaker constant. This interaction has no strong temperature dependence in contrast to experimental data (Fig. 4). The main contribution to $\tau_N-\tau_b$ is connected with interaction resulting from overlapping of smectic ordering from two surfaces [second term in Eq. (4)]. The energy of interaction between surfaces $F_{in}=\tau_N-\tau_b$ is negative. At low temperature $|F_{in}|$ reaches its maximum near the bulk transition temperature [15]. With increasing membrane thickness and temperature, the attractive interaction between surfaces $|F_{in}|$ strongly decreases (Fig. 4) due to decreasing smectic correlation length.

Up to now, no other measured quantities showed critical behavior near the thinning transitions. Based on the temperature dependence of the experimental data, one could not tell whether the membrane was near or far from the temperature of the thinning transition. As illustrated in Fig. 4, $|F_{in}|$ essentially decreases with heating when approaching the thinning transitions. Increase of the thinning transition temperature with decreasing membrane thickness occurs in accordance with behavior of $(\tau_N-\tau_b)/\tau$ for different membrane thicknesses. When, upon heating, the interaction energy $|F_{in}|$ decreases to some critical value (Fig. 4), the thinning transition occurs. We associate this energy with the lower bound of the surface interaction for membrane stability.

Thinning transitions are often associated with the mechanical instability of the layer structure [14]. The thinning should occur when the balance of the disjoining pressure and the elastic forces break down in the membrane. The elastic deformation concentrates in the membrane center, where the degree of smectic order is the lowest. The disjoining pressure ΔP_d is usually related to the curvature of the meniscus. It can be defined as the derivative of the free energy over the membrane thickness [15] or the work necessary to change the membrane thickness. This is the difference between air and membrane pressure, i.e., it is a pressure actually applied to the membrane. The second way to consider disjoining pressure is based on the difference between the free energy per layer at the surface of the membrane and in its interior [34,37]. The value defined in such a way, however, does not correspond to real pressure acting on the membrane. The physical reason for the stability of membranes may be explained as follows. Membranes are a metastable state of matter. At low temperatures, each membrane thickness corresponds to the local energy minimum associated with nonzero interaction between membrane surfaces. The membrane tension τ_N is less in thinner membranes, however, at low temperatures, the energetic barrier prevents the transition from the state with N to $N-1$ layers. At high temperatures, the interaction between the layers decreases, and inside the membrane a nonlayered structure may be formed. In this state, no energy is required to change the thickness of the film. In principle, the compound could enter the membrane from the meniscus forming a "quasismectic phase" [12]. However, this as a rule does not happen. Before the surface interaction reaches zero, a dislocation loop is formed in the membrane, which is followed by a thinning transition. As a result, the interaction of surfaces $|F_{in}|$ increases, and the energy of the film decreases. A driving force must exist for a thinning transition. Measurements of the droplet height H versus diameter D show nearly linear dependence for droplets with H much larger than the film thickness. This means that additional pressure in droplets with respect to air is smaller in larger droplets $\Delta P_d=2\tau_b/R\approx 8\tau_b H/D^2$. At the thinning transition due to the change of droplet shape (Fig. 2), the pressure ΔP_d increases about two times. Surface curvature in droplets (convex) and in meniscus (concave [15,38]) gives not only the different value of the pressure but even its sign. So the questions about the driving force of thinning and disjoining pressure remain open.

In summary, we have shown that the attractive surface interaction in the smectic membrane $|F_{in}|$ decreases with temperature, approaches zero near the thinning transition, and stepwisely increases after thinning. This behavior was predicted by de Gennes presmectic model. We used an internal membrane sensor—namely, droplets whose shape is very sensitive to interaction between the surfaces confining the presmectic membrane. The reason of the thinning transitions from the energetical point of view, in general, is clear but the nature of the driving force for thinning and dynamic phenomena are not yet fully understood. The interaction of surfaces in smectic membranes is much larger than in films of isotropic liquid and can be important up to several tens of nanometers. There are two contributions to the interaction induced by the smectic order parameter. The first one is the mean-field force. This interaction is oscillatory with respect to the mem-

brane thickness [22,39]. The second one is the attractive force induced by fluctuations of the smectic order (pseudo-Casimir force) [23,40]. However, the relative contribution of the mean-field and fluctuation-induced interaction to the total interaction of surfaces remains unknown. It should be noted also that most theories were developed for systems exhibiting second-order bulk phase transition, although most experiments were made using compounds with first-order transitions. Further studies of structure instability of smectic membranes, both theoretical and experimental, are required.

This work was supported in part by Russian Foundation for Basic Research, Grant No. 05-02-16675.

[1] P. Pieranski, L. Bieliard, J.-Ph. Tournelles, X. Leoncini, C. Furtlehner, H. Dumovlin, E. Rion, B. Jouvin, J.-P. Fénerol, Ph. Palaric, J. Heuving, B. Cartier, and I. Kraus, Physica A **194**, 364 (1993).
[2] W. H. de Jeu, B. I. Ostrovskii, A. N. Shalaginov, Rev. Mod. Phys. **75**, 181 (2003).
[3] T. Stoebe, P. Mach, and C. C. Huang, Phys. Rev. Lett. **73**, 1384 (1994).
[4] E. I. Demikhov, V. K. Dolganov, and K. P. Meletov, Phys. Rev. E **52**, R1285 (1995).
[5] V. K. Dolganov, E. I. Demikhov, R. Fouret, and C. Gors, Phys. Lett. A **220**, 242 (1996).
[6] S. Pankratz, P. M. Johnson, H. T. Nguyen, and C. C. Huang, Phys. Rev. E **58**, R2721 (1998).
[7] E. A. L. Mol, G. C. L. Wong, J. M. Petit, F. R. Rieutord, and W. H. de Jeu, Physica B **248**, 191 (1998).
[8] S. Pankratz, P. M. Johnson, R. Hołyst, and C. C. Huang, Phys. Rev. E **60**, R2456 (1999).
[9] S. Pankratz, P. M. Johnson, A. Paulson, and C. C. Huang, Phys. Rev. E **61**, 6689 (2000).
[10] P. Cluzeau, G. Joly, H. T. Nguyen, C. Gors, and V. K. Dolganov, Phys. Rev. E **62**, R5899 (2000).
[11] A. Zywocinski, F. Picano, P. Oswald, and J. C. Geminard, Phys. Rev. E **62**, 8133 (2000).
[12] L. V. Mirantsev, Phys. Lett. A **205**, 412 (1995).
[13] Y. Martinez-Raton, A. M. Somoza, L. Mederos, and D. E. Sullivan, Phys. Rev. E **55**, 2030 (1997).
[14] E. E. Gorodetskii, E. S. Pikina, and V. E. Podnek, Zh. Eksp. Teor. Fiz. **115**, 61 (1999) [JETP **88**, 35 (1999)].
[15] F. Picano, P. Oswald, and E. Kats, Phys. Rev. E **63**, 021705 (2001).
[16] A. N. Shalaginov and D. E. Sullivan, Phys. Rev. E **63**, 031704 (2001).
[17] L. V. Mirantsev, Phys. Rev. E **63**, 061701 (2001).
[18] A. N. Shalaginov and D. E. Sullivan, Phys. Rev. E **65**, 031715 (2002).
[19] A. Poniewierski, P. Oswald, and R. Hołyst, Langmuir **18**, 1511 (2002).
[20] B. M. Ocko, A. Braslau, P. S. Pershan, J. Als-Nielsen, and M. Deutsch, Phys. Rev. Lett. **57**, 94 (1986).
[21] G. S. Iannacchione, J. T. Mang, S. Kumar, and D. Finotello, Phys. Rev. Lett. **73**, 2708 (1994).
[22] P. G. de Gennes, Langmuir **6**, 1448 (1990).
[23] I. N. de Oliveira and M. L. Lyra, Phys. Rev. E **70**, 050702(R) (2004).
[24] P. Cluzeau, M. Ismaili, A. Anakhar, M. Foulon, A. Babeau, and H. T. Nguyen, Mol. Cryst. Liq. Cryst. Sci. Technol., Sect. A **362**, 185 (2001).
[25] M. Born and E. Wolf, *Principles of Optics* (Pergamon Press, New York, 1964).
[26] E. Demikhov and V. Dolganov, Ferroelectrics **181**, 179 (1996).
[27] P. Cluzeau, G. Joly, H. T. Nguyen, C. Gors, and V. K. Dolganov, Liq. Cryst. **29**, 505 (2002).
[28] P. Cluzeau, V. Bonnand, G. Joly, V. Dolganov, and H. T. Nguyen, Eur. Phys. J. E **10**, 231 (2003).
[29] H. Schuring and R. Stannarius, Langmuir **18**, 9735 (2002).
[30] P. Mach, C. C. Huang, T. Stoebe, E. D. Wedell, T. Nguyen, W. H. de Jeu, F. Guittard, J. Naciri, R. Shashidhar, N. Clark, I. M. Jiang, F. J. Kao, H. Liu, and H. Nohira, Langmuir **14**, 4330 (1998).
[31] M. Veum, C. Pettersen, P. Mach, P. A. Crowell, and C. C. Huang, Phys. Rev. E **61**, R2192 (2000).
[32] R. Jaquet and F. Schneider, Phys. Rev. E **67**, 021707 (2003).
[33] P. Oswald, F. Picano, and F. Caillier, Phys. Rev. E **68**, 061701 (2003).
[34] M. Veum, E. Kutschera, N. Voshell, S. T. Wang, S. L. Wang, H. T. Nguyen, and C. C. Huang, Phys. Rev. E **71**, 020701(R) (2005).
[35] Y. Martinez, A. M. Somoza, L. Mederos, and D. E. Sullivan, Phys. Rev. E **53**, 2466 (1996).
[36] J. Israelashvili, *Intermolecular and Surface Forces* (Academic Press, London, 1991).
[37] L. V. Mirantsev, Liq. Cryst. **20**, 417 (1996).
[38] J. C. Géminard, R. Hołyst, and P. Oswald, Phys. Rev. Lett. **78**, 1924 (1997).
[39] L. Moreau, P. Richetti, and P. Barois, Phys. Rev. Lett. **73**, 3556 (1994).
[40] P. Ziherl, Phys. Rev. E **61**, 4636 (2000).